Shear thinning of nanoparticle suspensions

Pieter J. in 't Veld,[1,2] Matt K. Petersen,[1] and Gary S. Grest[1]
[1]*Sandia National Laboratories, Albuquerque, New Mexico 87185, USA*
[2]*Polymer Research, BASF SE, 67056 Ludwigshafen, Germany*
(Received 9 July 2008; published 2 February 2009)

Results of large scale nonequilibrium molecular dynamics simulations are presented for nanoparticles in an explicit solvent. The nanoparticles are modeled as a uniform distribution of Lennard-Jones particles, while the solvent is represented by standard Lennard-Jones particles. We present results for the shear rheology of spherical nanoparticles of diameter 10 times that of the solvent for a range of nanoparticle volume fractions. By varying the strength of the interactions between nanoparticles and with the solvent, this system can be used to model colloidal gels and glasses as well as hard spherelike nanoparticles. Effect of including the solvent explictly is demonstrated by comparing the pair correlation function of nanoparticles to that in an implicit solvent. The shear rheology for dumbbell nanoparticles made of two fused spheres is similar to that of single nanoparticle.

DOI: 10.1103/PhysRevE.79.021401 PACS number(s): 83.80.Hj, 82.70.−y

The rheological properties of colloidal suspensions have been well studied [1]. For weakly interacting colloidal particles, the suspension is well described as a system of hard spheres, while increasing the interaction gives rise to colloidal gels and glasses. Since the size of the colloidal particle is much larger than the solvent, there is a clear separation of time and length scales between the colloidal particles and the solvent. This allows one to coarse grain the solvent and treat it as a continuum. However as the size of the colloidal particles are reduced to the range of what is now commonly referred to as nanoparticles, namely, 2–20 nm, treating the background implicitly is not adequate. For example, treating the solvent as a continuum does not account for local packing of the solvent around the nanoparticles, which can increase their effective radii. This can modify the effective interactions between nanoparticles, strongly affecting both the structure and dynamics of the suspension. To address such simple questions as to how large should the nanoparticles be to treat the solvent as a continuum or how do changes in the relative interactions between nanoparticles and between nanoparticles and the solvent affect the suspension rheology, it is important to develop a computationally tractable model of nanoparticle suspensions in which the solvent is treated explicitly.

Most models treat colloidal particles as hard spheres. However, this approach is not suitable for modeling colloids in an explicit solvent since hard spheres strongly phase separate even for relatively small differences in size [2]. Most hard sphere simulations have treated the solvent implicitly, usually by Brownian dynamics [3]. Stokesian dynamics [4] and related methods [5] include hydrodynamic interactions for the case of implicit solvent. Alternatively one can coarse grain the solvent by either lattice Boltzmann methods [6], dissipative particles [7] or stochastic rotational dynamics [8]. Each of these particle based methods introduces an effective coarse-graining length scale that is smaller than the colloids but much larger than the natural length scales of the solvent. None of them apply in the limit of interest here, namely, when the nanoparticles are comparable in size to the solvent.

To solvate the nanoparticles in an explicit solvent, it is critical to include an attractive component of the interaction between the nanoparticle and the solvent. The simplest effective potential is a Lennard-Jones (LJ) interaction shifted to the surface of the nanoparticle [9]. However, this potential does not capture the true interaction between nanoparticles as the range for which the interactions are important becomes increasingly small with increasing particle size. A more realistic approach is to treat each nanoparticle as being made of a uniform distribution of atoms, similar to treating them as a collection of atoms. In this case the effective potential can usually be determined analytically [10,11]. Integrated potentials are computational efficient, although the ability to freely choose shapes is traded for use of symmetrical shapes such as ellipsoids or spheres.

Here nanoparticles are assumed to consist of a uniform distribution of particles interacting with a Lennard-Jones interaction

$$U_{\mathrm{LJ}}(r) = 4\varepsilon_{nn}\left[\left(\frac{\sigma_n}{r}\right)^{12} - \left(\frac{\sigma_n}{r}\right)^{6}\right], \tag{1}$$

where r is the distance between two atoms. ϵ_{nn} is the interaction energy and σ_n is the diameter of the LJ atoms which make up each nanoparticle. For spherical nanoparticles, the total interaction between nanoparticles can then be determined analytically by integrating over all the interacting LJ atoms within the two particles [10]. The total interaction between nanoparticles $U_{nn}(r)=U^A_{nn}(r)+U^R_{nn}(r)$. $U^A_{nn}(r)$ is the standard attractive interaction between colloidal particles, first derived by Hamaker [12]. For particles of equal radii a,

$$U^A_{nn}(r) = -\frac{A_{nn}}{6}\left[\frac{2a^2}{r^2-4a^2} + \frac{2a^2}{r^2} + \ln\left(\frac{r^2-4a^2}{r^2}\right)\right]. \tag{2}$$

The Hamaker constant $A_{nn}=4\pi^2\epsilon_{nn}\rho_1\rho_2\sigma_n^6$, where ρ_1 and ρ_2 are the number density of LJ atoms within each sphere. The repulsive component of the interaction $U^R_{nn}(r)$ is [10]

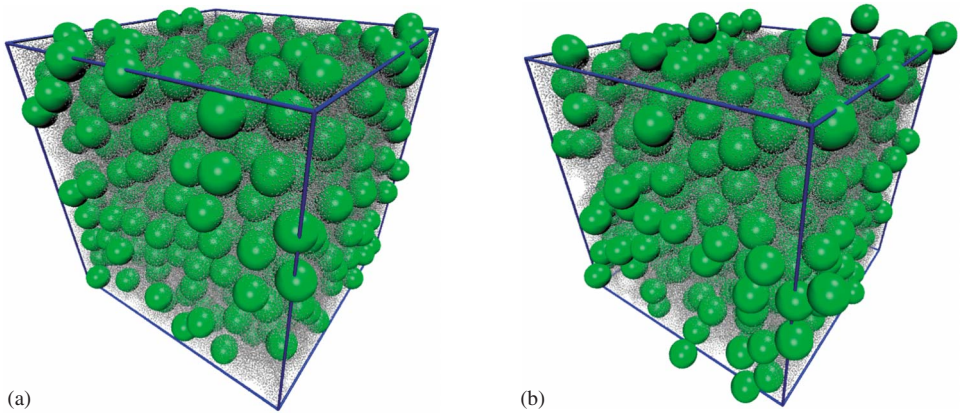

FIG. 1. (Color online) Sample simulation cell for $N=500$ nanoparticles of radii $a=5\sigma$ for $\phi_v=0.25$ in an explicit solvent for (a) monomers and (b) dimers. Solvent is shown as points.

$$U_{nn}^{R}(r)=\frac{A_{nn}}{37800}\frac{\sigma_n^6}{r}\left[\frac{r^2-14ra+54a^2}{(r-2a)^7}+\frac{r^2+14ra+54a^2}{(r+2a)^7}-\frac{2(r^2-30a^2)}{r^7}\right]. \quad (3)$$

Equations (2) and (3) reduce to the standard LJ potential, Eq. (1), in the limit $a\to 0$ and $\frac{4}{3}\pi a^3\rho_i=1$.

The interaction $U_{ns}(r)$ between the LJ solvent atoms and the nanoparticle is determined by integrating the interaction between a LJ solvent atom and the LJ atoms within the particle,

$$U_{ns}(r)=\frac{2a^3\sigma_{ns}^3A_{ns}}{9(a^2-r^2)^3}\left[1-\frac{(5a^6+45a^4r^2+63a^2r^4+15r^6)\sigma_{ns}^6}{15(a-r)^6(a+r)^6}\right], \quad (4)$$

where $A_{ns}=24\pi\epsilon_{ns}\rho_1\sigma_{ns}^3$. Here ϵ_{ns} is the interaction between a solvent atom and an atom in the nanoparticle and $\sigma_{ns}=(\sigma_n+\sigma_s)/2$, where σ_s is the size of a LJ solvent atom. The interaction between solvent atoms is the same Lennard-Jones interaction given in Eq. (1) with $\epsilon_{ss}=\epsilon$ and $\sigma_s=\sigma$. Note that, unlike most interaction potentials, $U_{nn}(r)$ and $U_{ns}(r)$ depend on both the size of the atoms making up the nanoparticle σ_n and the radii of the nanoparticle a.

Depending on the values of the Hamaker constant, the nanoparticles can either be dispersed in the solvent or aggregate. For nanoparticles made of the same Lennard-Jones atoms as the solvent ($\epsilon_{nn}=\epsilon_{ns}=\epsilon$ and $\sigma_n=\sigma$), we find that the nanoparticles and solvent phase separate for all values of the density ρ_1 of atoms which make up a nanoparticle. To solvate the nanoparticles, the interaction strength ϵ_{ns} has to be increased relative to ϵ_{nn}. For $\epsilon_{nn}=\epsilon$ simulations were run for several values of ϵ_{ns}. We found that $\epsilon_{ns}=3\epsilon$ was not sufficient to avoid phase separation, while $\epsilon_{ns}=6\epsilon$ was. As further increase of ϵ_{ns} gave an unphysical situation in which a layer or two of solvent atoms were attached to each nanoparticle, we chose to run all the simulations with $\epsilon_{ns}=6\epsilon$.

We chose to study three values for the nanoparticle/nanoparticle interaction strength. For the first, we considered that each nanoparticle was made of a LJ solid which has a density $\rho_1\sigma^3=1$. This gives $A_{nn}=4\pi^2\epsilon$ which corresponds to a very strong interaction between the solvent and the nanoparticles, resulting in a colloidal gel. For nanoparticles of the same density as the pure solvent $\rho_1\sigma^3=0.57$, the Hamaker constant is reduced significantly, $A_{nn}=12.9\epsilon$. However, in most nanoparticle suspensions, the nanoparticles are coated with short surfactants to avoid flocculation. This can be modeled by reducing A_{nn} further. For example, $A_{nn}=\epsilon$, as shown below, describes a hard spherelike nanoparticle suspension for $a=5\sigma$. For reference, the melting temperature for pure nanoparticles of radii $a=5\sigma$ is approximately $0.12-0.13A_{nn}$. Here we study how the structure and viscosity of the nanoparticle suspensions depend on the presence of the solvent for $a=5\sigma$.

All molecular dynamics simulations were performed using the LAMMPS simulation package [13]. Recent improvements to the algorithm [14], including multiregion neighbor lists and enhanced communications, have made the simulations presented here possible. For example, the speed up over previous versions of the code for nanoparticles of radii $a=10\sigma$ in an explicit solvent of LJ atoms is 200–400 times depending on nanoparticle concentration. Each configuration is prepared by combining a nanoparticle suspension in an implicit solvent with an equilibrated pure solvent of Lennard-Jones particles. The pure solvent and nanoparticle suspensions are merged by removing any solvent monomers that overlap a nanoparticle. This configuration is then equilibrated in an NPT ensemble for $T=\epsilon/k_B$ and $P=0.1\epsilon/\sigma^3$ to ensure a homogeneous suspension. The equilibrium simulations for the two pure systems are the same as in the case for the mixture, namely Newton's equations of motion were integrated using a velocity-Verlet algorithm coupled weakly to a heat bath [15] with a damping constant $\Gamma=0.01\tau^{-1}$. The integration time step $\delta t=0.005\tau$, where $\tau=\sigma(m/\epsilon)^{1/2}$. All results presented here are for an NVT ensemble. To ensure all the results are in equilibrium, at least 10^6 time steps were discarded at the beginning of each run. To reduce the number of parameters we set $\sigma_n=\sigma_s=\sigma$ and mass $m_n=\frac{4}{3}\pi a^3\rho_1 m$ with $\rho_1\sigma^3=1.0$ throughout, where m is the mass of the solvent.

The interactions between LJ atoms were cutoff at $r_c=3.0\sigma$, between nanoparticles at $5a$ and between LJ solvent atoms and nanoparticles at $a+4.0\sigma$. The number of nanoparticles varied from $N_n=40$ to 750 and LJ solvent atoms from a few thousand to six hundred thousand depending on the volume fraction $\phi_v=N_n\frac{4}{3}\pi a^3/V$ of nanoparticles. Note this definition of ϕ_v slightly underestimates the volume fraction since $U_{nn}(r)=0$ for $r=10.44\sigma>2a$ for $a=5\sigma$ unlike the case of two LJ monomers where $U_{\mathrm{LJ}}(r)=0$ for $r=\sigma$. However,

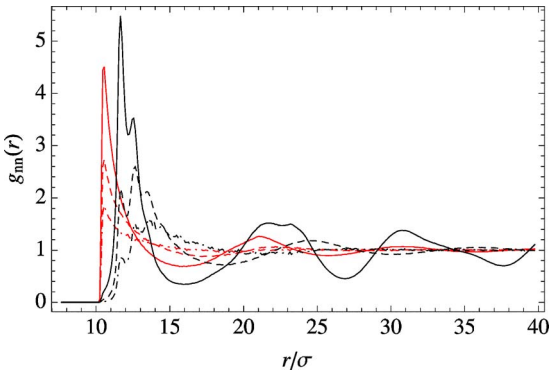

FIG. 2. (Color online) Nanoparticle-nanoparticle pair correlation functions $g(r)$ for nanoparticles of radii $a=5\sigma$ for volume fractions $\phi_v=0.12$ (dotted-dashed), 0.25 (dashed), and 0.39 (solid) for $A_{nn}=\epsilon$, $A_{ns}=72\epsilon$ with explicit solvent (black) and implicit solvent (red). The three curves for the implicit solvent are the ones with their first peak near $r\sigma\approx 10.4$.

since the separation r where $U_{nn}(r)=0$ depends on the nanoparticle radii a, this is a convenient definition. For the dimer system, pairs of nanoparticles are constrained to have a fixed bond length $b_n=\sigma$ using the SHAKE algorithm. Sample configurations for a monomer and dimer system for $a=5\sigma$ and $\phi_v=0.25$ are shown in Fig. 1. The nanoparticle suspensions were sheared with the SLLOD equations of motion [16] with a weak damping constant $\Gamma=0.01\tau^{-1}$.

The effect of including the solvent on the nanoparticle-nanoparticle pair correlations function $g_{nn}(r)$ is shown in Fig. 2 for the hard spherelike nanoparticles ($A_{nn}=\epsilon$) for an explicit and implicit solvent. Note that the first peak in $g(r)$ is higher for the explicit solvent and shifted to larger separations than for an implicit solvent. The solvent forms a layer near the nanoparticles, so that two nanoparticles cannot approach as closely as in the case of an implicit solvent, resulting in an effective nanoparticle radius which is greater than a. This result for the implicit solvent and the fact that the melting temperature for this case is approximately 0.12ϵ justifies our calling this case hard spherelike. Increasing Hamaker constants increases the correlations between nanoparticles and with the solvent. For the strongest interaction case $A_{nn}=4\pi^2\epsilon$, $A_{ns}=450\epsilon$, a layer of solvent particles are essentially bound to each nanoparticle resulting in an almost zero probability that two nanoparticles are ever closer than $\sim 12.2\sigma$. From visual observation of the configurations, these systems form a colloid gel with a nonuniform distribution of nanoparticles.

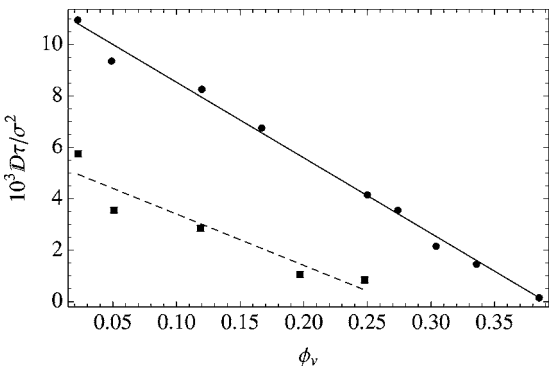

FIG. 3. Diffusion constant D versus volume fractions ϕ_v for radii $a=5\sigma$ for $A_{nn}=\epsilon$, $A_{ns}=72\epsilon$ (circles) and $A_{nn}=12.9\epsilon$, $A_{ns}=258\epsilon$ (squares).

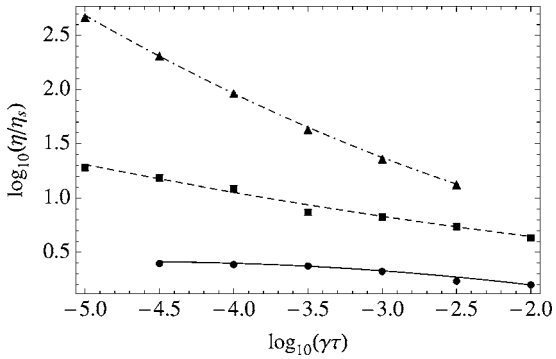

FIG. 4. Viscosity as a function of shear rate for volume fractions $\phi_v=0.25$ for radii $a=5\sigma$ for $A_{nn}=\epsilon$, $A_{ns}=72\epsilon$ (circles); $A_{nn}=12.9\epsilon$, $A_{ns}=258\epsilon$ (squares); and $A_{nn}=4\pi^2\epsilon$, $A_{ns}=450\epsilon$ (triangles).

The effect of varying the Hamaker constant on the diffusion constant D of the nanoparticles is shown in Fig. 3. The result for D at low concentrations is in agreement with the no slip Stokes-Einstein result $D=k_BT/(6\pi\eta_s a)=0.0105\sigma^2/\tau$, where $\eta_s=1.01\pm 0.03m/\tau\sigma$ is the viscosity of the pure solvent. The effect of varying the Hamaker constants on the shear rheology is shown in Fig. 4. Increasing interactions results in enhanced viscosity. For the strongest interacting case the suspension is in the shear thinning regime for all accessible shear rates.

In Fig. 5 we present results for a range of concentrations for hard spherelike monomers and dimers. Above $\phi_v\sim 0.39$ the monomer nanoparticle suspension crystallizes while the dimers do not. The liquid/solid transition point is slightly lower than for hard spheres ($\phi_v=0.494$). This is partially due to the fact that there is a weak interactions between the nanoparticles and underestimation of the volume fraction (radius). For the highest concentrations for the dimers there is evidence of a shear thickening regime. For $\phi_v\leqslant 0.34$, the viscosity reaches a plateau at low shear rates and we can extract

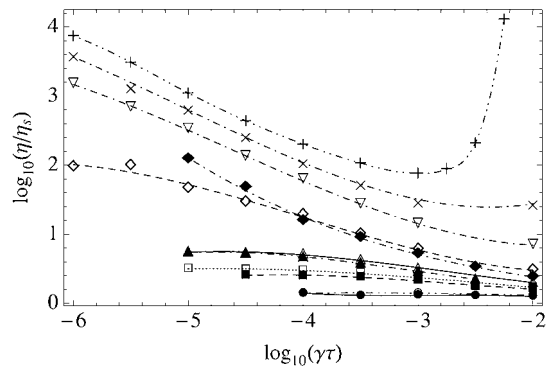

FIG. 5. Viscosity as a function of shear rate for monomers ($\phi_v\leqslant 0.39$) (closed) and dimers (open) for $A_{nn}=\epsilon$, $A_{ns}=72\epsilon$ for $\phi_v=0.12$ (circle), 0.25 (square), 0.31 (triangle), 0.39 (diamond), 0.49 (inverted triangle), 0.54 (cross), and 0.56 (plus).

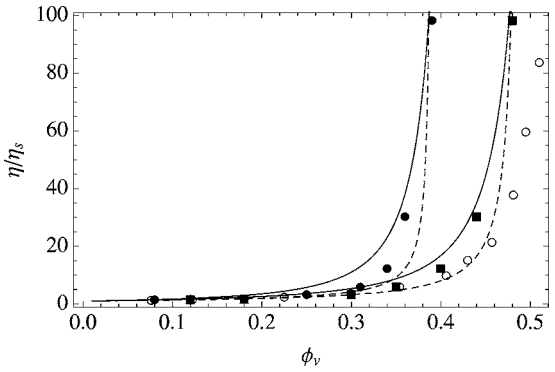

FIG. 6. Viscosity as a function of ϕ_v for hard-sphere-like dimers. The closed circles represent points assuming radii of $a=5\sigma$ in determining ϕ_v, whereas the squares denote the effective volume fraction for radii adjusted to the peak onset in the nanoparticle pair distribution function. The lines represent the best fit for the Quemada (solid) and Krieger Dougherty (dashed) expressions for each data set. Also shown are the experimental results for hard sphere colloids [17] (open circles).

the zero shear rate viscosity, which is shown in Fig. 6. Also shown are the experimental results for hard sphere colloids [17]. We fit the viscosity to the expressions of Krieger and Dougherty [18], $\eta/\eta_s=(1-\phi_v/\phi_c)^{-2.5\phi_c}$ and Quemada [19], $\eta/\eta_s=(1-\phi_v/\phi_c)^{-2}$. For hard sphere colloids, ϕ_c is between 0.57 and 0.63, the hard sphere glass transition and dense random packing fraction, respectively. Fitting the zero shear rate data to the Krieger Dougherty expression gives $\phi_c=0.39$, whereas the Quemada expression yields $\phi_c=0.43$. Clearly the fits severely underestimate ϕ_c. Since the nanoparticle-nanoparticle potential is nonzero at the defined nanoparticle radius ϕ_v slightly underestimates the volume fraction. Also as seen in Fig. 2 there is a weak solvation shell around the nanoparticles limiting the how close the nanoparticles approach each other, increasing the effective volume fraction especially for low ϕ_v. Adjusting the effective radii of the nanoparticle using the onset of the first peak in the nanoparticle pair correlation function, the best fit for $\phi_c=0.49$ and 0.53 for the Krieger-Dougherty and Quemada expressions, respectively.

Here we have presented a computationally tractable model for simulating nanoparticle suspensions in an explicit solvent. By varying the interaction between nanoparticles and with the solvent the model can be used to study colloidal gels and glasses as well as hard-sphere-like suspensions. Results of the simulations clearly show that including the solvent explicitly has important effects on both the structure and dynamics of nanoparticle suspensions. The minimum nanoparticle size at which the solvent can be treated as a continuum depends not only on the size of the nanoparticle but also the strength of the interaction A_{ns} between the nanoparticle and the solvent since it effects the size of the solvation shell around the nanoparticle. These two effects will be explored in future publications.

This work is supported by the Laboratory Directed Research and Development program at Sandia National Laboratories. Sandia is a multiprogram laboratory operated by Sandia Corporation, a Lockheed Martin Company, for the United States Department of Energy under Contract No. DE-AC04-94AL85000.

[1] W. B. Russel, D. A. Saville, and W. R. Schowalter, *Colloidal Dispersions*, 1st ed. (Cambridge University Press, Cambridge, 1989).
[2] M. Dijkstra, R. van Roij, and R. Evans, Phys. Rev. E **59**, 5744 (1999).
[3] D. L. Ermak and J. A. McCammon, J. Chem. Phys. **69**, 1352 (1978); D. R. Foss and J. F. Brady, J. Fluid Mech. **407**, 167 (2000); D. M. Heyes and H. Sigurgeirsson, J. Rheol. **48**, 223 (2004).
[4] J. F. Brady and G. Bossis, Annu. Rev. Fluid Mech. **20**, 111 (1988).
[5] R. C. Ball and J. R. Melrose, Jr., Adv. Colloid Interface Sci. **59**, 19 (1995); A. A. Catherall, J. R. Melrose, Jr., and R. C. Ball, J. Rheol. **44**, 1 (2000).
[6] A. J. C. Ladd and R. Verberg, J. Stat. Phys. **104**, 1191 (2001).
[7] P. J. Hoogerbrugge and J. M. V. A. Koelman, Europhys. Lett. **19**, 155 (1992); P. Espanol, Phys. Rev. E **57**, 2930 (1998); W. Dzwinel, K. Boryczko, and D. A. Yuen, J. Colloid Interface Sci. **258**, 163 (2003); V. Pryamitsyn and V. Ganesan, J. Chem. Phys. **122**, 104906 (2005).
[8] A. Malevanets and R. Kapral, J. Chem. Phys. **110**, 8605 (1999); **112**, 7260 (2000); M. Hecht, J. Harting, T. Ihle, and H. J. Herrmann, Phys. Rev. E **72**, 011408 (2005); J. T. Padding and A. A. Louis, *ibid.* **74**, 031402 (2006).
[9] M. J. Nuevo, J. J. Morales, and D. M. Heyes, Phys. Rev. E **58**, 5845 (1998); C. Powell, N. Fenwick, F. Bresme, and N. Quirke, Colloids Surf., A **206**, 241 (2002); D. Gersappe, Phys. Rev. Lett. **89**, 058301 (2002); S. R. Challa and F. van Swol, Phys. Rev. E **73**, 016306 (2006).
[10] R. Everaers and M. R. Ejtehadi, Phys. Rev. E **67**, 041710 (2003).
[11] T. Desai, P. Keblinski, and S. K. Kumar, J. Chem. Phys. **122**, 134910 (2005).
[12] H. C. Hamaker, Physica (Amsterdam) **4**, 1058 (1937).
[13] S. Plimpton, J. Comput. Phys. **117**, 1 (1995).
[14] P. J. in 't Veld, S. J. Plimpton, and G. S. Grest, Comput. Phys. Commun. **179**, 320 (2008).
[15] G. S. Grest and K. Kremer, Phys. Rev. A **33**, 3628 (1986).
[16] D. J. Evans and G. P. Morriss, Comput. Phys. Rep. **1**, 297 (1984); J. W. Rudisill and P. T. Cummings, Rheol. Acta **30**, 33 (1991); M. E. Tuckerman, C. J. Mundy, S. Balasubramanian, and M. L. Klein, J. Chem. Phys. **106**, 5615 (1997).
[17] S. P. Meeker, W. C. K. Poon, and P. N. Pusey, Phys. Rev. E **55**, 5718 (1997).
[18] I. M. Krieger and T. Dougherty, Trans. Soc. Rheol. **3**, 137 (1959).
[19] D. Quemada, Rheol. Acta **16**, 82 (1977).